



HAL
open science

Adaptive coupling of reduced basis modeling and Kriging based active learning methods for reliability analyses

Morgane Menz, Christian Gogu, Sylvain Dubreuil, Nathalie Bartoli, Jérôme Morio

► To cite this version:

Morgane Menz, Christian Gogu, Sylvain Dubreuil, Nathalie Bartoli, Jérôme Morio. Adaptive coupling of reduced basis modeling and Kriging based active learning methods for reliability analyses. 2020. hal-02405109v2

HAL Id: hal-02405109

<https://hal.science/hal-02405109v2>

Preprint submitted on 12 Feb 2020

HAL is a multi-disciplinary open access archive for the deposit and dissemination of scientific research documents, whether they are published or not. The documents may come from teaching and research institutions in France or abroad, or from public or private research centers.

L'archive ouverte pluridisciplinaire **HAL**, est destinée au dépôt et à la diffusion de documents scientifiques de niveau recherche, publiés ou non, émanant des établissements d'enseignement et de recherche français ou étrangers, des laboratoires publics ou privés.

Adaptive coupling of reduced basis modeling and kriging based active learning methods for reliability analyses

Morgane Menz^{a,b}, Christian Gogu^a, Sylvain Dubreuil^b, Nathalie Bartoli^b, Jérôme Morio^b

^a*Université de Toulouse, UPS, CNRS, INSA, Mines Albi, ISAE, Institut Clément Ader (ICA), 3 rue Caroline Aigle, 31400 Toulouse, France*

^b*ONERA/DTIS, Université de Toulouse, F-31055 Toulouse, France*

Abstract

Running a reliability analysis on engineering problems involving complex numerical models can be computationally very expensive. Hence advanced methods are required to reduce the number of calls to the expensive computer codes. Adaptive sampling based reliability analysis methods are one promising way to reduce the number of numerical model evaluations. Reduced order modelling is another one. In order to further reduce the numerical costs of kriging based adaptive sampling approaches, the idea developed in this paper consists in coupling both approaches by adaptively deciding whether to use reduced-basis solutions in place of full numerical solutions whenever the performance function needs to be assessed. Thus, a method combining such adaptive sampling based reliability analysis methods and reduced basis modeling is proposed based on an efficient coupling criterion. The proposed method enabled significant computational cost reductions while ensuring accurate estimations of failure probabilities.

Keywords: Reliability analysis, Kriging, Adaptive approaches, Finite elements, Reduced order modeling, Reduced basis

2010 MSC: 00-01, 99-00

1. Introduction

Reliability analyses is an efficient tool to deal with the numerous uncertainties present in engineering systems and thus determine the probability of failure of these systems. Many recent developments in this field seek to address increasingly complex numerical models, involving large physical and stochastic dimensions or even complex mechanical behaviors.

Generally speaking, a system failure mode is determined by a criterion from which a so called performance function G is defined. A negative value of this function corresponds to the failure of the system, whereas a positive value corresponds to an operational system. The limit between the failure and the safety domain is named limit state and corresponds to a null performance function. It thus allows the calculation of the probability of failure.

Several reliability analysis techniques exist to estimate the probability of failure such as analytic approximations (FORM/SORM), sampling methods [1], surrogate-based reliability analysis methods which can be adaptive or not. Adaptive approaches have been proposed in particular for Kriging surrogates [2] [3, 4, 5, 6, 7, 8], support vector machines [9, 10], Polynomial-Chaos-based Kriging in [11]. For a fixed sampling technique, the probability of failure is obtained by a classification of the samples, which is usually done by evaluating the numerical model at the corresponding samples. However, sometimes it may not be necessary to compute the full numerical model for all the samples, as many phenomena are very well described by a few dominant modes that can be accurately estimated based on adjacent samples. This is the basic idea of model order reduction approaches, which are used to reduce systems complexity while best preserving the system's response behaviour. In this paper, we focus on the model order reduction techniques known as reduced basis approaches or reduced order models by projection [12, 13]. These methods rely on the projection of the governing equations of the physical model involved onto a subspace of greatly reduced dimensionality compared to the initial space. Hence the resolution of the projected system involves a significantly reduced computational

cost. Following this concept, reduced basis techniques have already been combined with several reliability analysis techniques such as first or second-order reliability method or sampling based methods (i.e. Monte Carlo Simulations or even Importance Sampling) [14] [15] [16] [17] [18] and were shown to be able to lead to substantial computational savings. Presently, some of the most promising methods for reliability analysis are the ones based on an adaptive sampling approach. Kriging-based adaptive sampling methods [4] [19] [20] [21], which are also the object of this work, consist in building a Kriging surrogate model (Gaussian process interpolation) [22] of the performance function and using the uncertainty structure of Kriging to enrich iteratively this surrogate model. At each iteration of the algorithm, the best candidate for the next simulation is selected on the basis of a learning criterion and computed to increase the accuracy of the Kriging metamodel. This learning criterion is built to learn the limit state. In practice that means that the algorithm will enrich the metamodel in the vicinity of the currently known limit state and also explore the design space in less known areas, i.e. areas where the metamodel variance is high. To motivate our present work we can note that points in the vicinity of the limit state might be close to other points already evaluated and consequently the use of reduced-order solutions at these points are likely to have good accuracy while accelerating the method. Enrichment points in regions of high variance could also potentially benefit from reduced basis modelling, since these points can initially be calculated with the lower accuracy associated with reduced basis models, which may be enough to clarify the performance function's behaviour in these areas.

Accordingly the objective of this paper is to propose a reliability analysis method based on the coupling of adaptive sampling and reduced basis approaches. The proposed approach can thus be seen as an adaptive fidelity reliability analysis for the specific problems that are suitable for reduced basis modelling. The main challenge for setting up such an approach resides in defining an appropriate coupling criterion, based on which to decide whether the reduced basis models can be used or whether the accuracy of the full numerical

model is required. Different criteria based on a residual based error estimator will be investigated: one quite simple criterion but which can sometimes have poor accuracy and a preconditioning based criterion, which can potentially improve accuracy. The rest of the article is organized as follows. We present in Section 2 the problem statement. In Section 3 we provide a presentation of methods on which we build on such as an adaptive sampling based reliability analysis and, more precisely, the AK-MCS algorithm [19]. Section 3 also introduces the reduced-basis approach used in the present article. In Section 4 the new method combining adaptive sampling techniques and reduced-basis modeling is presented. First, we describe the overall framework of the proposed approach and then two implementations for the coupling of the algorithm AK-MCS with reduced-basis modeling are proposed, based on different coupling criteria. In Section 5 two application examples are considered. The first application concerns a reliability analysis on a thermal problem related to a regeneratively cooled combustion chamber. The second one is the estimation of the probability of failure of a laminated composite open hole plate based on the Tsai-Hill failure criterion. The performance of the proposed method is compared to the AK-MCS results and computational gains assessed.

2. Problem statement

This paper deals with reliability analyses involving certain numerically expensive models, specifically linear finite element models (e.g. in structural mechanics, heat exchange, etc). Let x_1, \dots, x_m be the m uncertain parameters that are input to the finite element model. These parameters are modeled by an absolutely continuous random vector X of random variables X_i , $i = 1, \dots, m$ characterized by a probability distribution with probability density function f_X . The output of the numerical model $Y(X)$ is then also a random variable. After finite element discretization of the equilibrium equation and the application of boundary conditions the following linear system of \mathcal{N} degrees of freedom is

typically obtained:

$$K(x)u(x) = F(x) \quad (1)$$

where K is an $\mathcal{N} \times \mathcal{N}$ matrix (called stiffness matrix in structural mechanics), $u \in \mathbb{R}^{\mathcal{N}}$ the vector of the unknown state variables (e.g. displacements in structural mechanics, temperatures in heat exchange, etc) and $F \in \mathbb{R}^{\mathcal{N}}$ the vector of loadings (e.g. applied forces in structural mechanics, heat fluxes in heat transfer). In the context of reliability, the output of interest is the performance function G , which is considered here dependent on the state variable $u(x)$, solution of the finite element model:

$$G(x) = G(u(x), x) \quad (2)$$

The performance function $G : \mathbb{R}^m \rightarrow \mathbb{R}$ characterizes the failure of a structure. Hence the domain of failure reads $\mathcal{D}_f = \{x \in \mathbb{R}^m, G(x) \leq 0\}$, the domain of safety reads $\{x \in \mathbb{R}^m, G(x) > 0\}$ and the limit state is $\{x \in \mathbb{R}^m, G(x) = 0\}$. The failure probability P_f is then defined as:

$$P_f = \int_{\mathbb{R}^m} \mathbb{1}_{G(x) \leq 0} f_X(x) dx \quad (3)$$

Several methods exist to obtain an estimation of this probability. One of the simplest method is Monte Carlo Simulation (MCS). It consists in simulating a random independent and identically distributed sample of size n_{MC} with distribution f_X and then classifying this population given the value taken by the performance function. An estimation \hat{P}_f of the failure probability P_f is then given by:

$$\hat{P}_{f_{MC}} = \frac{1}{n_{MC}} \sum_{i=1}^{n_{MC}} \mathbb{1}_{G \leq 0}(x^i) \quad (4)$$

where $(x^1, \dots, x^{n_{MC}})$ corresponds to the Monte Carlo sample. The following estimation of the coefficient of variation can be used to quantify the uncertainty of the estimated failure probability:

$$\widehat{COV}_{P_f_{MC}} = \sqrt{\frac{(1 - \hat{P}_{f_{MC}})}{n_{MC} \hat{P}_{f_{MC}}}} \quad (5)$$

It can be seen on Eq. (5) that for a failure probability of 10^{-n} , 10^{n+2} simulations are needed to obtain an estimated coefficient of variation of about 10%. The computational cost may thus be very important for computationally expensive functions G . In the next section, an alternative approach based on adaptive
85 sampling is presented.

3. Adaptive sampling based reliability analysis methods and Reduced-Basis Modeling

3.1. Reliability analysis using a Kriging surrogate model

Sampling based classification methods need a lot of simulations to estimate
90 the failure probability. In order to avoid to evaluate a complex performance function G on a whole Monte Carlo population, an approximation by a surrogate model of this function \hat{G} can be used instead. However the accuracy of the surrogate model needs to be controlled in the regions near the limit state in order to allow an accurate classification of the Monte Carlo points in these
95 areas. For this purpose, Kriging based adaptive sampling methods allow to construct and enrich a Kriging metamodel by using the uncertainty structure of this type of surrogate models to adaptively add learning points in regions that contribute significantly to the probability of failure estimate. More specifically, these methods use learning functions to select the best point to evaluate i.e. the
100 one which would improve the metamodel in the vicinity of the limit state.

3.1.1. The Kriging surrogate model

Kriging, introduced in geostatistics by Krige [23] and formalized later by Georges Matheron [24], is a method of interpolation in which the interpolated function is modeled by a Gaussian process. For a dataset $\{G(x), x = (x^1, \dots, x^n)\}$ Kriging or Gaussian Process [22] is fully characterized by the Kriging mean $\mu(x)$ and a kernel (or covariance function) $C(x^i, x^j)$ and can be defined as:

$$\hat{G}(x) = \mu(x) + Z(x) \quad (6)$$

with:

- the Kriging mean $\mu(x) = \phi(x)\beta$ with $\phi(x)$ a basis functions vector and β the associated regression coefficients.
- $Z(x)$ a stationary zero mean Gaussian process with the variance σ_Z^2 such that the kernel defining the Kriging is

$$C(x^i, x^j) = \text{cov}(\hat{G}(x^i), \hat{G}(x^j)) = \sigma_Z \Psi(x^i, x^j, \theta),$$

105 Ψ being a user defined correlation function type.

Finally, σ_Z , β and the hyperparameters θ must be estimated to approximate the response for any unknown point of the domain. For a fixed kernel type, several techniques exist to obtain the optimal values of these hyperparameters, for example by Maximum Likelihood Estimation [25] or cross-validation [22].

110 Now consider a zero mean Gaussian process \hat{G} , i.e. $\mu(x) = 0$. The distribution of the Kriging prediction for an unknown point x^* , taking into account the a priori distribution of the observations, is Gaussian with the mean and variance given by the expressions:

$$\mu_{\hat{G}}(x^*) = K(x^*, x)K(x, x)^{-1}y \quad (7)$$

$$\sigma_{\hat{G}}^2(x^*) = K(x^*, x^*) - K(x^*, x)K(x, x)^{-1}K(x, x^*) \quad (8)$$

with $K : (x, x^*) \rightarrow K(x, x^*)$ the covariance matrix such that $K(x, x^*)_{ij} = C(x_i, x_j^*)$.

115 In the following section, the adaptive sampling reliability analysis method AK-MCS, which combines Kriging and Monte Carlo based Simulation, will be presented.

3.1.2. AK-MCS

The active learning reliability method combining Kriging and Monte Carlo Simulation (AK-MCS) is an adaptive reliability estimation method proposed
120 by Echard et al. [19], based on the interpolation of the performance function by Kriging together with the use of a specific learning function and on the Monte Carlo method. This method aims to classify a Monte Carlo population

125 S without evaluating each sample with the numerically expensive performance
function. The different stages of AK-MCS are summarized in Fig. 1 and de-
scribed below:

1. Generation of an initial Monte Carlo population S of n_{MC} samples.
2. Initial Design of Experiments (DoE) D of n samples defined using sam-
130 pling methods such as Latin Hypercube Sampling (LHS). The performance
function G is then evaluated for the n samples.
3. Construction of a Kriging metamodel \hat{G} of the performance function G on
the DoE.
4. Estimation of the failure probability P_f on the Monte Carlo population S
according to the following equation:

$$\hat{P}_{f_{AK-MCS}} \approx \frac{n_{\hat{G} \leq 0}}{n_{MC}} \quad (9)$$

5. The learning function U given in Eq. (10) is evaluated on the whole pop-
ulation S to find the best candidate to evaluate for enriching the Kriging
metamodel.

$$U(x) = \frac{|\mu_{\hat{G}}(x)|}{\sigma_{\hat{G}}(x)} \quad (10)$$

with $\mu_{\hat{G}}(x)$ and $\sigma_{\hat{G}}(x)$ respectively the mean and standard deviation of
the Kriging model of \hat{G} (see Eq. (7) and Eq. (8)).

6. If the learning stopping criterion defined by Eq. (11) is fulfilled the meta-
model is considered sufficiently accurate for the population S and the
active learning is stopped. Then the algorithm goes to step 8. Otherwise,
the algorithm goes to step 7.

$$\min_{x \in S} U(x) \geq 2 \quad (11)$$

7. The performance function is computed on the sample minimizing the
135 learning function U and the DoE is enriched with this new point x^* . Then
the algorithm goes back to step 3.
8. The estimated value of the coefficient of variation (COV) on the probabil-
ity of failure $\widehat{COV}_{P_f_{AK-MCS}}$ is verified to ensure the consistency of the

Monte Carlo Simulations. In case the COV is too high, new samples are added to the Monte Carlo population used in AK-MCS and the method goes back to step 7. Otherwise, if the COV is below a user defined threshold the failure probability obtained with the AK-MCS method is the final estimation.

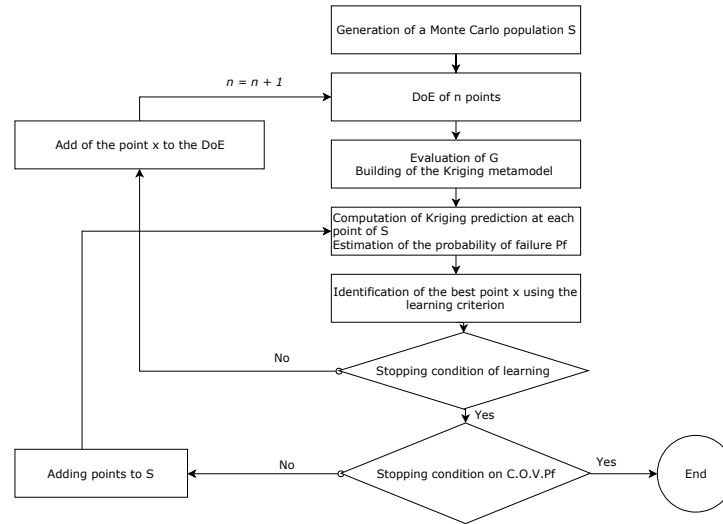


Figure 1: Flowchart of the AK-MCS Algorithm.

One can note that step 7 of the AK-MCS algorithm involves the resolution of the numerical model. Given the finite element models we consider here (of the form given in Eq. (1)), the idea pursued in the present article is to reduce the numerical cost of this step (and thus the whole reliability analysis) by applying model order reduction method to the resolution of Eq. (1) and to use the obtained approximate solution in the AK-MCS algorithm if this approximation

reaches a given accuracy threshold. To this purpose, next Section introduces the retained reduce basis approach.

3.2. Reduced-Basis Modeling

Model order reduction is a technique for decreasing the computational cost associated to the resolution of a full order model in numerical simulations, i.e. decrease the cost associated with the resolution of the system of Eq. (1). One of the existing model order reduction approaches, which will be considered in this work, is reduced-basis modelling or reduced-order modeling by projection. This method aims at solving the system of equations (1) by projection onto a reduced basis denoted $\Phi = (\Phi_1, \dots, \Phi_{n_{RB}})$, where Φ_i , $i = 1, \dots, n_{RB} \in \mathbb{R}^{\mathcal{N}}$. The initial problem projected on the reduced basis Φ is then rewritten:

$$\Phi^T K(x) \Phi \alpha(x) = \Phi^T F(x) \quad (12)$$

where $\alpha \in \mathbb{R}^{n_{RB}}$ are the coefficients of the state vector u expressed in the reduced basis Φ . Thus the new problem to solve is a linear system of $n_{RB} \ll \mathcal{N}$ equations. Indeed the projected problem involves the inversion of the projected stiffness matrix $\Phi^T K \Phi \in \mathbb{R}^{n_{RB} \times n_{RB}}$ and provides after resolution the vector α . We should note that the projected matrix size is very low compared to the size of the initial stiffness matrix which can reach millions of dof (degrees of freedom) for large-scale finite elements problems. On the other hand, it was found empirically and is generally accepted in the reduced order modelling community [12], that the size of an acceptable reduced basis is in the order of a few dozen for a large variety of engineering problems. The reduced solution is then obtained as $\tilde{u} = \Phi \alpha$. In practice, the exact error between the reduced solution and the real one is not computed (since it would defeat any computational savings) but the accuracy associated to the reduced basis solution can be estimated by the following residual [15]:

$$\epsilon_{RB} = \frac{\|K \Phi \alpha - F\|_2}{\|F\|_2} \quad (13)$$

So far, the reduced basis Φ , on which the problem is projected, was not specified
 155 as many methods exist to define a projection subspace. In this paper, an on-the-

fly method [26], which will be described in details in the next section, is used to construct the reduced basis. Indeed, this method is well suited to the combination with active learning as it consists in enriching the reduced basis iteratively along the sequential reliability estimation procedure with all the simulations for which the full solution of the system Eq. (1) was computed. In practice, both for the construction of the reduced-basis and for the computation of the residual, the stiffness matrix K needs to be assembled. The computational cost of this operation can be non negligible in general, however, for large-scaled problems it becomes increasingly negligible compared with solving the system Eq. (1). Besides the assembly of the matrix K , the computation of the residual ϵ_{RB} only involves matrix-vector products and differences whose computational costs are also insignificant for problems of large dimensions. Model order reduction is thus a powerful technique to reduce computational time and its use within the AK-MCS approach is proposed in the following.

4. Proposed Method

4.1. General concept

We propose here an hybrid reliability analysis method coupling active learning approaches and reduced-basis modeling. Indeed, some points of the DoE may not need to be evaluated using the full numerical simulations. Points located close to the limit state might be in the vicinity of other infill points which have previously been computed (using the full order model) and consequently reduced-order solutions at these points are likely to have good accuracy. The proposed procedure starts with the definition of an initial DoE which at the same time serves to initialize both the surrogate model and the reduced basis. In fact, the first point of the DoE is evaluated with the full numerical model and is considered as the first element of the reduced basis. At each point of the DoE, the response of the reduced-basis model and a criterion on the accuracy of the reduced solution are computed. Then, based on the accuracy criterion it is decided either to use the reduced solution or to solve the full order model. In

185 this case the solution computed using the full order is also used to enrich the
reduced basis Φ . A surrogate is then fitted using both reduced and complete
solutions. At each iteration of the learning phase the same operations are car-
ried out to evaluate the infill points. In the next sections the method combining
the algorithm AK-MCS and reduced basis modeling with different criteria is
190 described.

4.2. Coupling of AK-MCS and reduced-basis modeling

We propose here an algorithm combining the method AK-MCS and reduced
basis modeling based on the framework presented in the previous sections. It
involves to take in consideration reduced solutions in the initialization and learn-
195 ing phases of AK-MCS. The algorithm of the proposed method is provided in
Algorithm 1 and described below. The algorithm starts with the initialization
of the reduced basis. Therefore, the first sample of the initial DoE is computed
and normalized to serve as the first element Φ_1 of the reduced basis. Then all
other samples of the DoE, i.e. samples of the initial DoE and infill points added
200 in the learning phase, are evaluated according to the following steps:

1. Computation of the reduced solution \tilde{u}_i at the point x^i by projection on
the available reduced basis.
2. Computation of the residual ϵ_{RB} for the previous solution based on Eq. (13).
3. Evaluation of the accuracy of the solution \tilde{u}_i . If the value of ϵ_{RB} is below a
205 user defined threshold ϵ , the reduced solution is considered to be accurate
enough and is added to the DoE. Otherwise, go to next step.
4. If the reduced solution is found not to be accurate enough based on the
previous threshold, the full numerical problem is solved. The associated
result u_i is added to the DoE and also used to enrich the reduced basis
210 after orthonormalization as shown in Eq. (14) and (15).

$$\Phi_i = u_i - \sum_{k=1}^{i-1} \langle u_i, \Phi_k \rangle \Phi_k \quad (14)$$

$$\Phi_i = \frac{\Phi_i}{\|\Phi_i\|_2} \quad (15)$$

with $\langle \cdot, \cdot \rangle$ the L^2 scalar product.

The proposed method adaptively makes the choice of using reduced-basis solutions or the full numerical model. This coupling can thus greatly reduce the execution time of AK-MCS since the computation of reduced solutions and residuals are less expensive than the resolution of the full finite element problem.

4.3. Coupling of AK-MCS and reduced-basis modeling with preconditioned residuals

While the residuals of Eq. (13) can be used as a first estimation of the accuracy of the reduced basis solution it may be insufficiently accurate in some cases, depending in particular on the conditioning number of the stiffness matrix. Furthermore, it may not be easy to decide on a threshold based on the relative residual of Eq. (13) which is defined on the loading vector, as one is more interested in the relative error on the state variable vector (e.g. displacement vector). The use of a preconditioner P can thus improve the error estimators based on the residuals [27] as the preconditioned residual is homogeneous to the state variable. Thus, the following preconditioned residual is also considered in this section:

$$\epsilon_{RB}^P = \frac{\|P^{-1}K\Phi\alpha - P^{-1}F\|_2}{\|P^{-1}F\|_2} \quad (16)$$

The computation of the preconditioned residual ϵ_{RB}^P is in general more expensive than the computation of ϵ_{RB} due to the computation of the term $P^{-1}K\Phi\alpha$. However for preconditioners that are independent of the parameter x , the decomposition of P can be stored once for all. Thus the only cost is the resolution of the system according to the type of factorization chosen, which has to be done in any case, and which thus does not induces any significant additional

Algorithm 1: Coupling algorithm

Generate a Monte Carlo population S of size n_{MC}

Define an initial DoE D of n samples

$u \leftarrow$ solution of $K(x^1)u(x^1) = F(x^1)$

$y_{doe} \leftarrow G(u, x^1)$

for $x \in D \setminus \{x^1\}$ **do**

- $\alpha \leftarrow$ solution of $\Phi^T K(x)\Phi\alpha(x) = \Phi^T F(x); \quad u \leftarrow \Phi\alpha$
- $\epsilon_{RB} \leftarrow \frac{\|K\Phi\alpha - F\|_2}{\|F\|_2}$
- if** $\epsilon_{RB} > \epsilon$ **then**
 - $u \leftarrow$ solution of $K(x)u(x) = F(x)$
 - $V \leftarrow u - \Phi(\Phi^T u); \quad \Phi \leftarrow [\Phi, \frac{V}{\|V\|_2}]$
- $y_{doe} \leftarrow [y_{doe}, G(u, x)]$

while $COV < 10\%$ **do**

- while** *learning stopping criterion not reached* **do**
 - Fit Kriging model \hat{G} with (D, y_{doe})
 - $\hat{Y}, \sigma_Y \leftarrow \hat{G}(x), \forall x \in S$
 - $P_f \leftarrow \frac{n_{\hat{G} \leq 0}}{n_{MC}}; \quad COV \leftarrow \sqrt{\frac{1 - P_f}{P_f \cdot n_{MC}}}$
 - $U_{learning} \leftarrow \frac{|\hat{Y}|}{\sigma_Y}$
 - $x \leftarrow \arg \min_{x' \in S} U_{learning}(x')$
 - if** $U_{learning}(x) < 2$ **then**
 - $\alpha \leftarrow$ solution of $\Phi^T K(x)\Phi\alpha(x) = \Phi^T F(x); \quad u \leftarrow \Phi\alpha$
 - $\epsilon_{RB} \leftarrow \frac{\|K\Phi\alpha - F\|_2}{\|F\|_2}$
 - if** $\epsilon_{RB} > \epsilon$ **then**
 - $u \leftarrow$ solution of $K(x)u(x) = F(x)$
 - $V \leftarrow u - \Phi(\Phi^T u); \quad \Phi \leftarrow [\Phi, \frac{V}{\|V\|_2}]$
 - $D \leftarrow [D, x]; \quad y_{doe} \leftarrow [y_{doe}, G(u, x)]$
 - else**
 - \perp learning stopping criterion reached
- Generate a Monte Carlo population S^* of size n_{MC}
- $S \leftarrow [S, S^*]$

End of algorithm

computational cost. Hence the previously proposed method for coupling AK-
 225 MCS and reduced basis modeling can be improved by using the preconditioned
 residual ϵ_{RB}^P in order to improve the residual based error estimation used to
 decide if the reduced solution is accurate enough to be used in place of the full
 numerical solution. There exist several ways of constructing a preconditioner.
 In this paper, the proposed method will be run with two possible preconditioner
 230 construction techniques:

- the mean point preconditioner [28]: the full numerical model is computed
 at the mean point of the physical design space and the resulting matrix
 K^0 serves as preconditioner $P = K^0$.
- the nearest point preconditioner: every time the full numerical model is
 235 computed to enrich the reduced basis, the matrix $K^i = K(x^i)$ is stored to
 serve as a possible preconditioner (let us denote $\mathcal{X}_{full} = \{x^i, i = 1, \dots, n_{full}\} \subset S$
 which contains the point where the full solution has been computed).
 Then, for each sample evaluation, at point $x^* \notin S$, the preconditioned
 residual is computed using $P = K^i$ where $x^i = \min_{x \in \mathcal{X}_{full}} \|x - x^*\|_2$.

240 The two proposed strategies coupling AK-MCS and reduced-basis modeling with
 or without the use of a preconditioner are numerically investigated to compare
 their performances on two applications. The first one concerns a thermal prob-
 lem and the second one a mechanical problem.

5. Applications

245 In the following, the two numerical applications are presented. For each one
 a description of the physical problem is given followed by the numerical com-
 parisons between the different strategies to estimate the probability of failure.

5.1. First application example: Reliability analysis on a thermal problem

5.1.1. Description of the problem

250 In this section, the application considered is a reliability analysis, which in-
 volves the heat transfer through the combustion chamber wall of a regeneratively

cooled rocket engine [29, 30, 15]. In such an engine, liquid hydrogen (LH2) flow-
 ing through cooling channels in the combustion chamber wall at a temperature
 of 40K is used for cooling the engine. We consider that failure occurs when the
 maximum temperature of the inner wall of the combustion chamber exceeds a
 critical value T_{allow} , which corresponds to the cooling channel walls rupture.

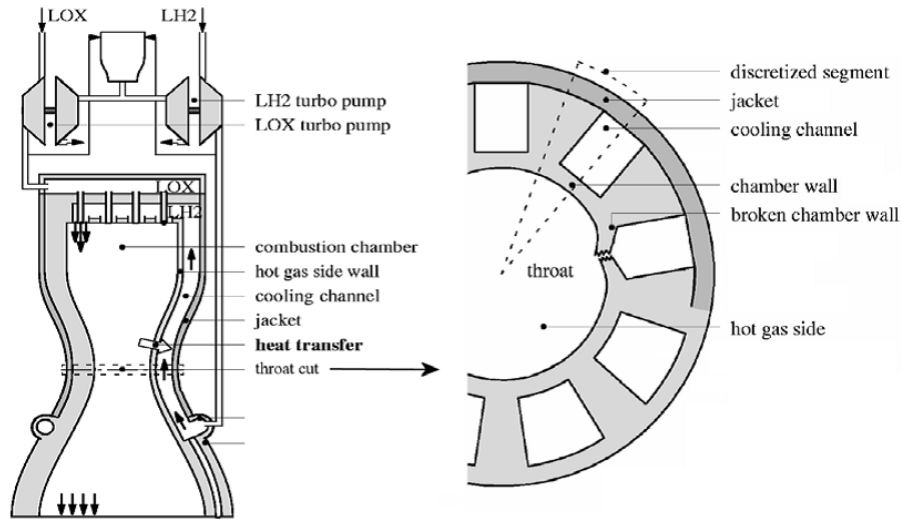


Figure 2: Schematic of a regeneratively cooled rocket engine combustion chamber.

A schematic of the combustion chamber of a typical regeneratively cooled
 liquid hydrogen (LH2) liquid oxygen (LOX) rocket engine is shown on Fig. 2.
 As illustrated on this figure, two different parts made of two different materials
 form the combustion chamber wall: an internal side made of a copper alloy and
 an external jacket made of a Ni alloy. Heat exchanges may happen through
 convection between the combustion chamber wall and the sources of heat (com-
 bustion chamber gases) and cooling (liquid hydrogen) and also with the exterior.
 Considering these boundary conditions, the resulting thermal transfer depends
 of the following parameters: the conductivity of the inner side of the wall (k_{Cu}),
 the conductivity of the jacket (k_{Ni}), the temperature of the gases on the inner
 side of the combustion chamber (T_{hot}), the film convection coefficient on the in-
 ner side of the combustion chamber (h_{hot}), the temperature on the outer side of

the combustion chamber (T_{out}), the film convection coefficient on the outer side
of the combustion chamber (h_{out}), the temperature of the cooling fluid (T_{cool})
and the film convection coefficient on the cooling channel side (h_{cool}). These
parameters and the maximum temperature allowable T_{allow} are supposed to be
uncertain and are modeled by independent random variables following proba-
bility distributions given in Table 1. Thermal field at stationary equilibrium
is obtained by resolution of a convection-diffusion equation by a finite element
approach. The finite element mesh of the combustion chamber wall and the
boundary conditions are illustrated in Fig. 3.

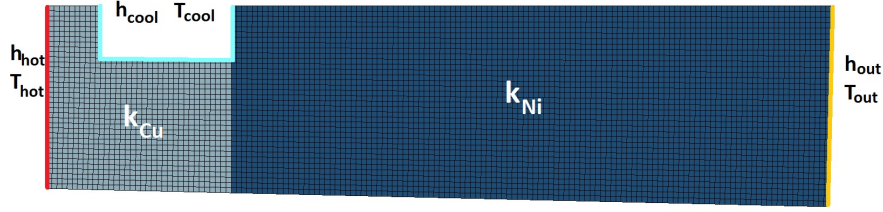


Figure 3: Finite element mesh of the combustion chamber wall and the boundary conditions of the thermal problem.

Input	k_{Cu}	k_{Ni}	T_{hot}	h_{hot}	T_{out}	h_{out}	T_{cool}	h_{cool}	T_{allow}
Unit	W/mK	W/mK	K	kW/m^2K	K	kW/m^2K	K	kW/m^2K	K
Probability law	Gaussian	Gaussian	Uniform	Uniform	Uniform	Uniform	Uniform	Uniform	Uniform
Mean	310	75	900	31	293	6	40	250	230
COV	2%	2%							
Half-range			10%	10%	5%	5%	5%	10%	7.5%

Table 1: Probability distributions of the thermal problem parameters.

Here an in-house finite element solver coded in Python is used to compute the thermal field. Thus we have access to the maximum temperature and we can deduce the performance function, defined here as $G(x) = T_{allow}(x) - T_{max}(x)$. Then the failure probability can be estimated using Monte Carlo sampling or using AK-MCS based strategies. The results of these comparisons are presented in the following.

5.1.2. Results

First, a Monte Carlo Simulation was run to have an accurate estimation of the failure probability used as reference in the following comparison. The estimation obtained with standard Monte Carlo was $\hat{P}_{fMC} = 6.22 \cdot 10^{-3}$ with an estimated COV of 5.65% (for $n_{MC} = 5 \times 10^4$). The AK-MCS method was implemented using the reduced-basis coupling with the classical and the mean point preconditioned residual criteria. These two methods were run on the same thermal problem described in the previous section. In order to verify the residual is a valid coupling criterion, the Pearson correlation coefficient between the residual and the *real error* is estimated (*real error* is defined as the error between the reduced solution and the finite element solution). The samples used for this estimation are the points used during the construction of the reduced basis by Algo. 1. As depicted on Fig. 4, the preconditioned residual is almost perfectly correlated to the real error, which can be explained by the well-posedness of the problem. The correlation between the real error and the non preconditioned residual has a lower score but seems to be quite good for very small errors under 5×10^{-3} .

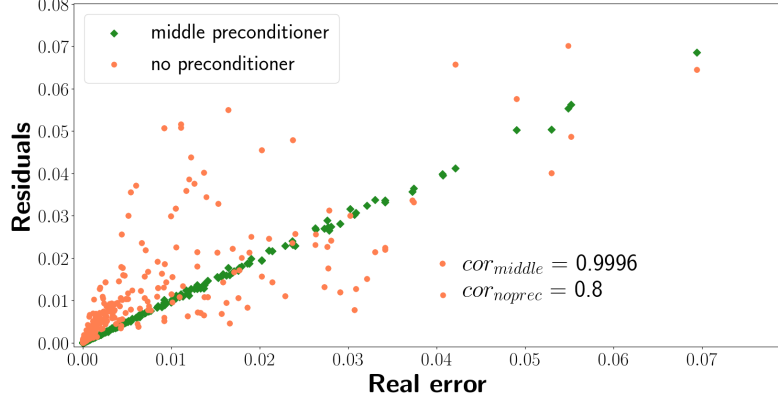


Figure 4: Correlation between the residuals and the real error for the thermal problem.

The graphical representation of the first three modes of a temperature reduced basis constructed on-the-fly during a run of the coupling based on ϵ_{RB} for $\epsilon = 10^{-3}$ is given in Fig. 5. The construction methodology used implies that the first mode is the dominant mode, meaning that it is the one that represents the best the typical thermal fields. However, to capture finer variations of the thermal field and thus achieve accurate reduced solutions, additional basis vectors (corresponding to additional modes) are needed. Therefore it is interesting to study the influence of the value ϵ taken as threshold for the coupling criterion on the proposed method's performances. To this end, the following procedure is carried out:

- Run AK-MCS algorithm and save the resulting DoE (i.e. initial DoE and infill points)
- For varying threshold ϵ , apply the reduced basis coupling on the samples of the AK-MCS DoE in the same order they were added by AK-MCS algorithm.

Here two criteria are used to compare the proposed method performances for different ϵ :

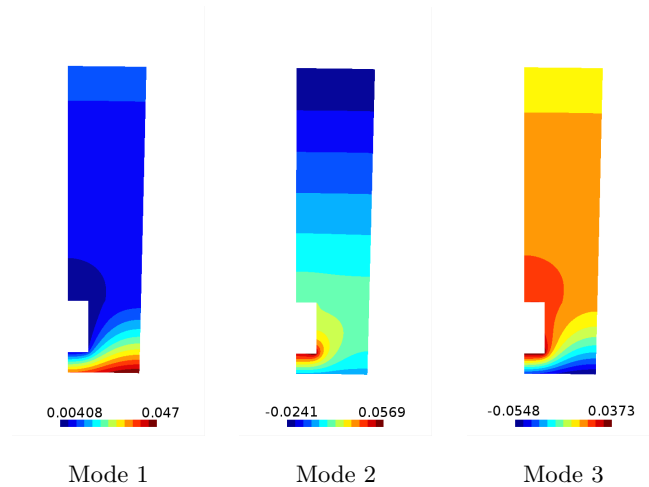


Figure 5: First three temperature modes obtained using the on-the-fly constructing procedure through AK-MCS for the thermal problem.

- the speed up achieved by using the proposed method over AK-MCS, i.e. the ratio of number of evaluations of the full numerical model in AK-MCS to the number of its evaluations when using the coupling. Note that we only compare the ratios of the full numerical models, as the cost of inverting the reduced basis model becomes negligible as the size (number of degrees of freedom) of the problem increases.
- the relative accuracy of the failure probability estimation. Here we compare the estimations of $\widehat{P}_{f_{AK-MCS+RB}}$ and $\widehat{P}_{f_{AK-MCS}}$ on the same initial DoE and Monte Carlo population. The relative accuracy is thus defined by the formula $1 - \frac{|\widehat{P}_{f_{AK-MCS}} - \widehat{P}_{f_{AK-MCS+RB}}|}{\widehat{P}_{f_{AK-MCS}}}$ where a perfect accuracy will have a value equals to 1.

In order to take into account the stochastic variation of the AK-MCS approach in the assessment of the influence of the parameter ϵ , the previous procedure was run 10 times for different initial DoEs and Monte Carlo populations. The mean of the two criteria described just above were thus computed for different values of the threshold. Their evolution is given on Fig. 6 for the non preconditioned

residual ϵ_{RB} and on Fig. 7 for the preconditioned residual ϵ_{RB}^P .

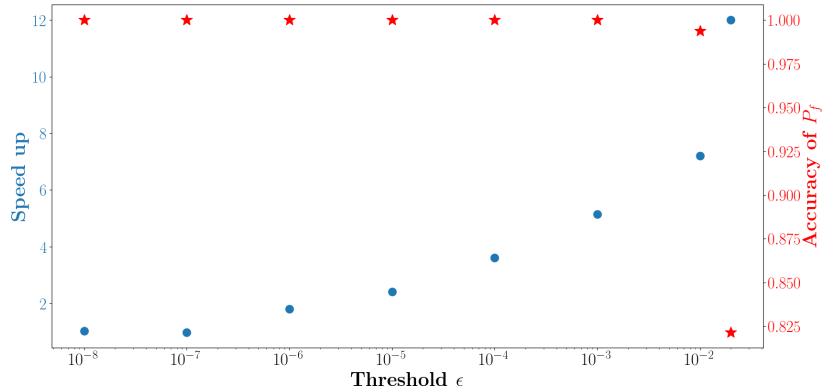


Figure 6: Accuracy (red stars) of P_f and speed up (blue dots) of the proposed method as a function of the threshold ϵ on the non preconditioned residual for different constant DoEs and Monte Carlo generated by AK-MCS algorithm for the thermal problem.

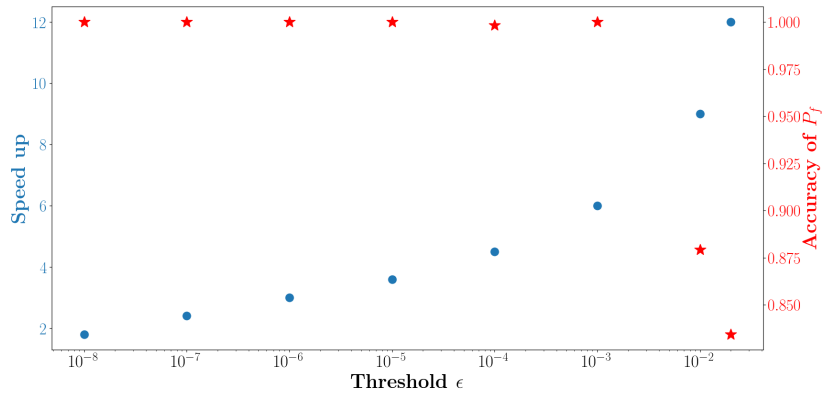


Figure 7: Accuracy (red stars) of P_f and speed up (blue dots) of the proposed method as a function of the threshold ϵ on the preconditioned residuals for different constant DoEs and Monte Carlo generated by AK-MCS algorithm for the thermal problem.

335 From these figures a good compromise between speed up obtained by the proposed algorithm and accuracy of the probability of failure estimate results seems to be reached for $\epsilon = 10^{-3}$. It can also be noted that even if the cor-

relation of the real error with the non preconditioned residual is not as good as if preconditioning is used (as shown by Fig. 4), it is sufficient here to obtain satisfying results in terms of estimating the probability of failure. On the basis of these results, AK-MCS and the proposed methods are now compared in more details for $\epsilon = 10^{-3}$. Compared to the previous study, one should note that, in the proposed approach, the selection of enrichment points is now potentially led by the solution obtained using the reduced basis approximation. For each version of the proposed methods (with and without preconditioning) 30 computations of both the proposed method and AK-MCS for a same initial DoE and Monte Carlo population have been run. The sample mean \overline{P}_f and corrected sample standard deviation $\overline{\sigma}_{P_f}$ based on the results of these runs can be found on Table 2 and Table 3.

	\overline{P}_f	$\overline{\sigma}_{P_f}$
AK-MCS	6.52×10^{-3}	1.88×10^{-4}
AK-MCS + RB	6.52×10^{-3}	1.90×10^{-4}

Table 2: Mean results of AK-MCS and AK-MCS + RB with no preconditioned residual for the thermal problem.

	\overline{P}_f	$\overline{\sigma}_{P_f}$
AK-MCS	6.52×10^{-3}	1.88×10^{-4}
AK-MCS + RB	6.52×10^{-3}	1.88×10^{-4}

Table 3: Mean results of AK-MCS and AK-MCS + RB with preconditioned residual for the thermal problem.

First of all, note that the sample means obtained for the AK-MCS algorithm and for the proposed method are consistent with the Monte-Carlo reference $\hat{P}_{f_{MC}} = 6.22 \cdot 10^{-3}$ (with an estimated COV of 5.65%). More precisely, the sample mean obtained for both proposed method variants are very close to the AK-MCS reference $\widehat{P}_{f_{AK-MCS}}$ sample mean. Note as well that the values of the

355 estimated variances don't take extreme values when the reduced basis is used
and are even very close to the reference $\widehat{\sigma}_{\widehat{P}_{f_{AK-MCS}}}$, especially for the preconditioned residual strategy. For these computations the speed up of the algorithm in terms of full numerical simulations is of 6.372 for the preconditioned residual strategy and of 5.736 for the non preconditioned residual strategy. Moreover,
360 for a run of the coupling algorithm with and without preconditioning full evaluations represent on average respectively 29.4% and 36.1% of the total number of evaluations, corresponding respectively to 6.7 basis vectors out of 38.1 evaluated samples and 6 basis vectors out of 40.66 evaluated samples in average.

To confirm these promising results, a second, numerically more complex
365 application is investigated in the following.

5.2. Second application example: failure of a bending composite laminate plate with a hole

5.2.1. Description of the problem

We now consider the application of the proposed methods on a mechanical problem involving a potentially non-symmetric laminates, due to uncertainties in the ply layup. The test case illustrated on Fig. 8 is the reliability analysis of a laminated plate with a hole under under uniform vertical pressure considering the Tsai-Hill failure criterion recalled below:

$$\left(\frac{\sigma_L(\theta, h)}{X_{ult}}\right)^2 + \left(\frac{\sigma_T(\theta, h)}{Y_{ult}}\right)^2 + \left(\frac{\tau_{LT}(\theta, h)}{\tau_{ult}}\right)^2 - \frac{\sigma_L(\theta, h)\sigma_T(\theta, h)}{X_{ult}^2} > 1 \quad (17)$$

where X_{ult} , Y_{ult} and τ_{ult} are the ultimate strengths and σ_L , σ_T and τ_{LT} are
370 respectively the longitudinal, transverse and shear stresses. The variables θ and h are respectively the fiber orientation angles and the ply thickness for each of the six plies of the laminate. It is assumed that, due to manufacturing uncertainties, these parameters are random and thus are modeled by the following independent random variables:

- the ply thicknesses h_i follow gamma distributions $\Gamma(\mu, \sigma, \gamma)$ with parameters provided in Table 4,

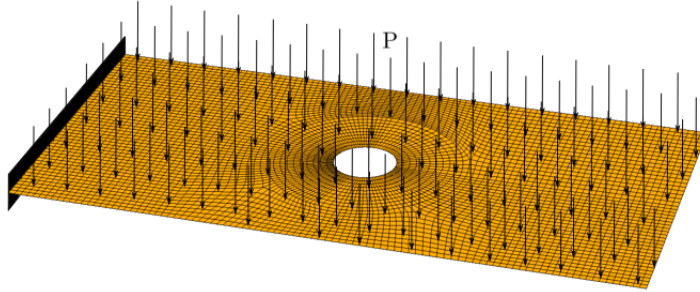


Figure 8: Boundary conditions and loading on the laminated plate.

- the fiber orientation angles θ_i follow uniform distributions $\mathcal{U}(a, b)$ with parameters provided in Table 5.

μ	$2 \cdot 10^{-4}$
σ	$2 \cdot 10^{-5}$
γ	0

Table 4: Parameters of the gamma probability distribution used to model all ply thicknesses.

	θ_1	θ_2	θ_3	θ_4	θ_5	θ_6
a	-2.5	42.5	-47.5	-47.5	42.5	-2.5
b	2.5	47.5	-42.5	-42.5	47.5	2.5

Table 5: Parameters of the uniform probability distributions used to model the fiber orientation angles.

Note that the nominal laminate is thus assumed to have a ply thickness of
 380 0.2 mm and a layup of $[0, 45, -45]_s$. However due to uncertainties, the actual
 laminate may have different values, in particular it is non-symmetric in general.
 A MATLAB-based in-house finite element solver is used here to compute the
 stress field. We used a four-node Mindlin shell element with five degrees of

freedom per node with a shear correction factor computed according to [31].

385 The finite element mesh of the laminate used here is illustrated in Fig. 9. The elastic constants of a ply are provided in Table 6. The longitudinal ultimate tensile and compression strengths (resp. X_{ult}^T and X_{ult}^C), transversal ultimate tensile and compression strengths (resp. Y_{ult}^T and Y_{ult}^C) and ultimate in-plane shear strength (τ_{ult}) of the ply are provided in Table 7.

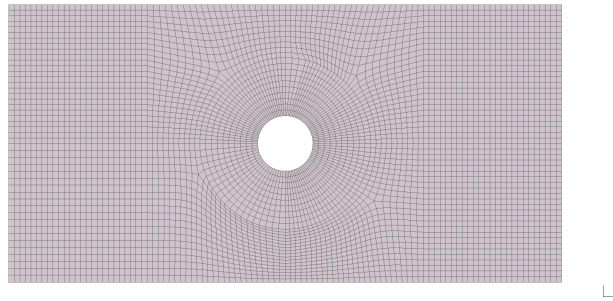


Figure 9: Finite element mesh of the laminated plate with a hole.

E_1	E_2	ν_{12}	G_{12}
181 GPa	10.3 GPa	0.28	7.17 GPa

Table 6: Ply elastic constants.

X_{ult}^T	X_{ult}^C	Y_{ult}^T	Y_{ult}^C	τ_{ult}
997 MPa	847 MPa	38 MPa	198 MPa	60 MPa

Table 7: Ply ultimate stresses.

390 In the next section, the failure probability will be estimated using AK-MCS and reliability analysis based on the proposed strategy in order to test the performances of the coupling on the presented problem.

5.2.2. Results

First, a Monte Carlo Simulation was run to have an accurate estimation of the failure probability of this problem. The estimation obtained with standard
 395 Monte Carlo was $\hat{P}_{f_{MC}} = 5.4 \cdot 10^{-4}$ with an estimated COV of 9.62% (for $n_{MC} = 2 \times 10^5$).

Then, a similar study as the one for the thermal problem was carried on this problem. First the correlation between the residuals and the real error
 400 was estimated. Figure 10 presents the correlation when the residual is not preconditioned. It can be seen on this figure that the coefficient of correlation between the non preconditioned residual and the real error is very low and that many residuals take values greater than 1. This is probably due to the higher ill-conditioning of this problem, compared to the previous one, in particular due
 405 to the non symmetric laminates that are considered, inducing bending-shear coupling. On the basis on these results, it would be quite hard to find an efficient threshold ϵ and ensure the effectiveness of the coupling.

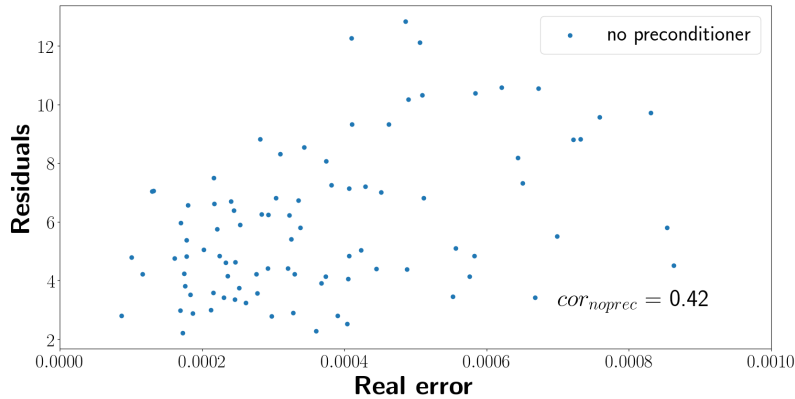


Figure 10: Correlation between the classical residual and the real error for the plate with a hole problem.

Hence the correlation with preconditioned residuals was considered next. Given the higher numerical complexity of this application, both precondition-
 410 ers presented in Section 4.3 were tested. As seen in Fig. 11, the two proposed

preconditioners have similar performances for this problem and the coefficients of correlation are almost equal to 0.96 which is a significant improvement compared to non preconditioned residual ($cor_{noprec} = 0.42$). For these reasons, the following computations with the proposed method will be run using the mean point preconditioner to evaluate the residuals.

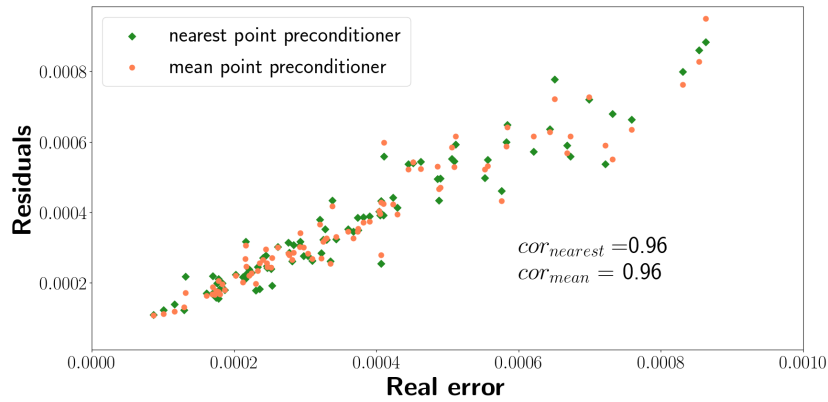


Figure 11: Correlation between the preconditioned residuals and the real error for the laminated plate with a hole problem.

As in the thermal problem, the first modes of the displacement field constructed on-the-fly during a run of the coupling, based on ϵ_{RB}^P for $\epsilon = 10^{-3}$, can be graphically represented. The representations of the four first basis vectors of the displacement field in the out of plane direction are given in Fig. 12. The first mode has obviously much similarity with the general shape of the displacement field, which again is asymmetric, due to the non-symmetric laminates and induced bending shear coupling. For this same reason, the higher modes represented describe even more complex variations of the displacement fields. Hence, due to this relatively complex behaviour it can be expected that more modes will be required on this application to satisfy the error criterion $\epsilon = 10^{-3}$.

The performance of the proposed methods for different thresholds on ϵ_{RB}^P was studied next, following the same process as for the first application, i.e. using the coupling strategy on a fixed DoE generated during a run of AK-MCS

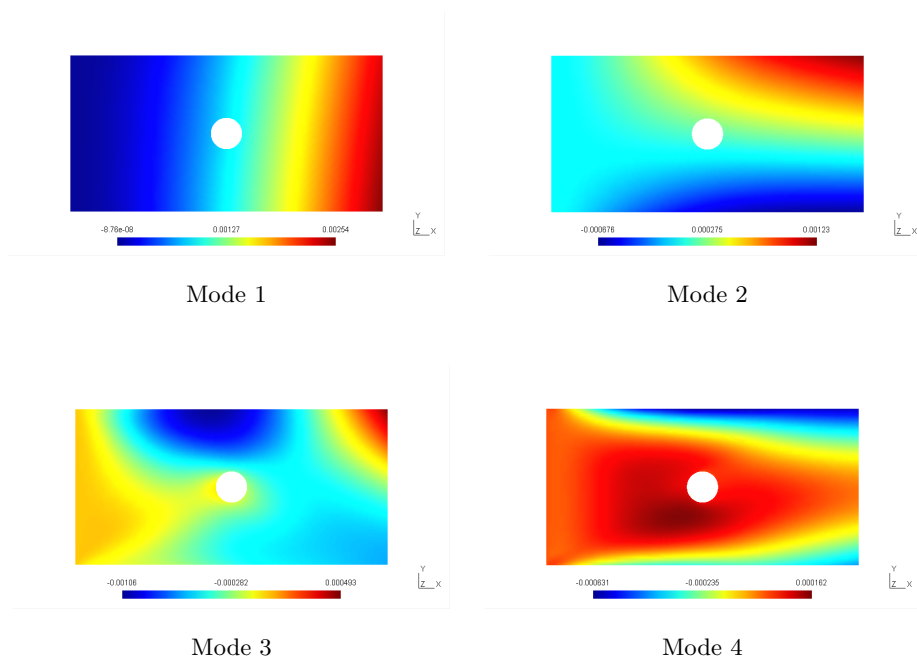


Figure 12: First four Z-displacement modes obtained using the on-the-fly constructing procedure through AK-MCS for the laminated plate with a hole problem.

for varying thresholds. The mean values of the speed up and accuracy computed
 430 over 10 runs as a function of ϵ are given on Fig. 13.

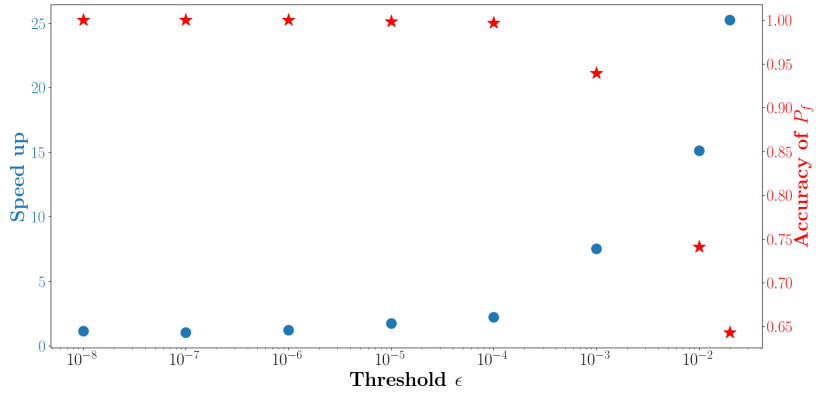


Figure 13: Accuracy (red stars) of the failure probability P_f and speed up (blue dots) as a function of the threshold ϵ on the preconditioned residuals for different constant DoEs and Monte Carlo generated by AK-MCS algorithm for the laminated plate with a hole problem.

According to Fig. 13 the best compromise between accurate estimations and a consequent acceleration of the reliability analysis method lies again at $\epsilon = 10^{-3}$. Then AK-MCS and the proposed method were run 40 times for different initial DoEs and Monte Carlo populations with $\epsilon = 10^{-3}$. The resulting
 435 sample means $\overline{P_f}$ and corrected sample standard deviation $\overline{\sigma_{P_f}}$ are given in Table 8. The mean failure probability estimated by the proposed method is in the 95% confidence interval of the mean results of AK-MCS $[4.39 \times 10^{-4}, 4.85 \times 10^{-4}]$. Moreover the corrected sample standard deviations are in the same order of magnitude whether reduced basis solutions are used or not. On average, the use of
 440 the proposed methods over AK-MCS allows a speed-up of 7.1. Furthermore, for a run of the coupling algorithm full numerical evaluations represent on average only 16.4% of the total number of evaluations, corresponding to 14.35 basis vectors out of 111.15 evaluated samples on average.

	\overline{P}_f	$\overline{\sigma_{P_f}}$
AK-MCS	4.62×10^{-4}	4.94×10^{-5}
AK-MCS + RB	4.47×10^{-4}	5.19×10^{-5}

Table 8: Mean results of AK-MCS and AK-MCS + RB with preconditioned residual for the laminated plate with a hole problem.

6. Conclusions

445 The present article proposes strategies to improve the efficiency of adaptive sampling surrogate based reliability analysis techniques based on the use of reduced basis solutions over expensive full numerical solutions, made possible by an adaptive construction of an efficient reduced basis. The proposed approach first initializes a reduced basis during the initial phase of the active learning

450 algorithm. Then, based on a reduced solution accuracy criterion it decides for each point either to use the reduced solution or to solve the full numerical model. As the learning phase of the adaptive sampling concentrates the choice of infill points in the vicinity of the limit state, reduced-basis modeling may be very efficient as new points are likely to be close to many already computed points.

455 Two different implementations of the approach were proposed, differing in terms of the reduced basis coupling criterion. The applications have highlighted the limitations on a criterion based on a basic residual and the usefulness of an improved criterion based on a preconditioned residual. The performance of the proposed approach was also assessed on the two applications, which have shown

460 that the coupling has a great potential of reducing the computational costs. The speed up is of course dependent of the problem, but on the application problems considered the speed up reached up to a factor of 7.1. A perspective to improve the coupling criterion is to look at the exploration phase during the learning. Indeed, according to the current definition of the criterion, infill points

465 in less known area are likely to be evaluated using the full numerical model as they are located far from other points. However to clarify the behaviour of

the performance function in less known area due to a high variance reduced solutions may be sufficient in a first step. This consideration could be taken into account in the coupling criterion and may be the subject of a later work.

⁴⁷⁰ **Acknowledgment**

This work was supported by the French National Research Agency (ANR) through the ReBReD project under grant ANR-16-CE10-0002.

References

- [1] R. E. Melchers, A. T. Beck, Structural Reliability Analysis and Prediction, John Wiley & Sons, 2018, google-Books-ID: 8yE6DwAAQBAJ. 475
- [2] E. Vazquez, J. Bect, A Sequential Bayesian algorithm to estimate a probability of failure, in: 15th IFAC, Symposium on System Identification (SYSID'09), 5 pages, Saint-Malo, France, July 6-8, 2009.
- [3] B. Echard, N. Gayton, M. Lemaire, N. Relun, A combined Importance Sampling and Kriging reliability method for small failure probabilities with time-demanding numerical models, Reliability Engineering & System Safety 111 (Supplement C) (2013) 232–240. doi:10.1016/j.ress.2012.10.008. 480
URL <http://www.sciencedirect.com/science/article/pii/S0951832012002086> 485
- [4] B. J. Bichon, M. S. Eldred, L. P. Swiler, S. Mahadevan, J. M. McFarland, Efficient Global Reliability Analysis for Nonlinear Implicit Performance Functions, AIAA Journal 46 (10) (2008) 2459–2468. doi:10.2514/1.34321. 490
URL <http://arc.aiaa.org/doi/10.2514/1.34321>
- [5] B. J. Bichon, J. M. McFarland, S. Mahadevan, Efficient surrogate models for reliability analysis of systems with multiple failure modes, Reliability Engineering & System Safety 96 (10) (2011) 1386–1395. doi:10.1016/j.ress.2011.05.008. 495
URL <http://www.sciencedirect.com/science/article/pii/S0951832011001062>
- [6] W. Fauriat, N. Gayton, AK-SYS: An adaptation of the AK-MCS method for system reliability, Reliability Engineering & System Safety 123 (2014) 137–144. doi:10.1016/j.ress.2013.10.010. 500
URL <http://www.sciencedirect.com/science/article/pii/S0951832013002949>

- [7] L. Li, J. Bect, E. Vazquez, Bayesian Subset Simulation: a Kriging-based subset simulation algorithm for the estimation of small probabilities of failure, in: Proceedings of PSAM 11 and ESREL 2012, 25-29 June 2012, Helsinki, Finland, 2012.
- 505
- [8] V. Dubourg, E. Deheeger, B. Sudret, Metamodel-based importance sampling for the simulation of rare events, in: Faber, M. J. Kohler and K. Nishilima (Eds.), Proceedings of the 11th International Conference of Statistics and Probability in Civil Engineering (ICASP2011), Zurich, Switzerland, 2011.
- 510
- [9] A. Basudhar, S. Missoum, Reliability assessment using probabilistic support vector machines, International Journal of Reliability and Safety 7 (2) (2013) 156–173. doi:10.1504/IJRS.2013.056378.
URL <https://www.inderscienceonline.com/doi/abs/10.1504/IJRS.2013.056378>
- 515
- [10] J. M. Bourinet, F. Deheeger, M. Lemaire, Assessing small failure probabilities by combined subset simulation and Support Vector Machines, Structural Safety 33 (6) (2011) 343–353. doi:10.1016/j.strusafe.2011.06.001.
URL <http://www.sciencedirect.com/science/article/pii/S0167473011000555>
- 520
- [11] Schbi R., Sudret B., Marelli S., Rare Event Estimation Using Polynomial-Chaos Kriging, ASCE-ASME Journal of Risk and Uncertainty in Engineering Systems, Part A: Civil Engineering 3 (2) (2017) D4016002. doi:10.1061/AJRUA6.0000870.
URL <https://ascelibrary.org/doi/abs/10.1061/AJRUA6.0000870>
- 525
- [12] P. Benner, S. Gugercin, K. Willcox, A Survey of Projection-Based Model Reduction Methods for Parametric Dynamical Systems, SIAM Review 57 (4) (2015) 483–531. doi:10.1137/130932715.
URL <http://epubs.siam.org/doi/abs/10.1137/130932715>
- 530

- [13] G. Kerschen, J.-C. Golinval, A. F. Vakakis, L. A. Bergman, The Method of Proper Orthogonal Decomposition for Dynamical Characterization and Order Reduction of Mechanical Systems: An Overview, *Nonlinear Dynamics* 41 (1-3) (2005) 147–169. doi:10.1007/s11071-005-2803-2.
535 URL <https://link.springer.com/article/10.1007/s11071-005-2803-2>
- [14] R. E. Melchers, Importance sampling in structural systems, *Structural Safety* 6 (1) (1989) 3–10. doi:10.1016/0167-4730(89)90003-9.
URL <http://www.sciencedirect.com/science/article/pii/0167473089900039>
540
- [15] C. Gogu, A. Chaudhuri, C. Bes, How Adaptively Constructed Reduced Order Models Can Benefit Sampling-Based Methods for Reliability Analyses, *International Journal of Reliability, Quality and Safety Engineering* 23 (05) (2016) 1650019.
- 545 [16] E. Florentin, P. Dez, Adaptive reduced basis strategy based on goal oriented error assessment for stochastic problems, *Computer methods in applied mechanics and engineering* 225-228 (2012) 116–127. doi:10.1016/j.cma.2012.03.016.
URL <https://upcommons.upc.edu/handle/2117/116664>
- 550 [17] S. Boyaval, C. L. Bris, Y. Maday, N. C. Nguyen, A. T. Patera, A reduced basis approach for variational problems with stochastic parameters: Application to heat conduction with variable Robin coefficient, *Computer Methods in Applied Mechanics and Engineering* 198 (41-44) 3187–3206.
URL http://www.academia.edu/27337716/A_reduced_basis_approach_for_variational_problems_with_stochastic_parameters_Application_to_heat_conduction_with_variable_Robin_coefficient
555
- [18] J. Bect, D. Ginsbourger, L. Li, V. Picheny, E. Vazquez, Sequential design of computer experiments for the estimation of a prob-

- 560 ability of failure, *Statistics and Computing* 22 (3) (2012) 773–793.
doi:10.1007/s11222-011-9241-4.
URL <https://link.springer.com/article/10.1007/s11222-011-9241-4>
- [19] B. Echard, N. Gayton, M. Lemaire, AK-MCS: An active learning reliability
565 method combining Kriging and Monte Carlo Simulation, *Structural Safety*
33 (2) (2011) 145–154. doi:10.1016/j.strusafe.2011.01.002.
URL <http://www.sciencedirect.com/science/article/pii/S0167473011000038>
- [20] V. Dubourg, B. Sudret, J.-M. Bourinet, Reliability-based Design Optimiza-
570 tion Using Kriging Surrogates and Subset Simulation, *Struct. Multidiscip.*
Optim. 44 (5) (2011) 673–690. doi:10.1007/s00158-011-0653-8.
URL <http://dx.doi.org/10.1007/s00158-011-0653-8>
- [21] M. Balesdent, J. Morio, J. Marzat, Kriging-based adaptive Importance
575 Sampling algorithms for rare event estimation, *Structural Safety* 44 (Sup-
plement C) (2013) 1–10. doi:10.1016/j.strusafe.2013.04.001.
URL <http://www.sciencedirect.com/science/article/pii/S0167473013000350>
- [22] C. E. Rasmussen, C. K. I. Williams, Gaussian processes for machine learn-
580 ing, *Adaptive computation and machine learning*, MIT Press, Cambridge,
Mass, 2006, oCLC: ocm61285753.
- [23] D. G. Krige, A statistical approach to some basic mine valuation problems
on the Witwatersrand, *Journal of the Southern African Institute of Mining
and Metallurgy* 52 (6) (1951) 119–139.
URL https://journals.co.za/content/saimm/52/6/AJA0038223X_4792
585 4792
- [24] G. Matheron, Principles of geostatistics, *Economic Geology* 58 (8) (1963)
1246–1266. doi:10.2113/gsecongeo.58.8.1246.

URL <https://pubs.geoscienceworld.org/segweb/economicgeology/article-abstract/58/8/1246/17275/principles-of-geostatistics>

- 590 [25] D. R. Jones, A Taxonomy of Global Optimization Methods Based on Response Surfaces, *Journal of Global Optimization* 21 (4) (2001) 345–383. doi:10.1023/A:1012771025575.

URL <https://doi.org/10.1023/A:1012771025575>

- [26] C. Gogu, J.-C. Passieux, Efficient surrogate construction by combining response surface methodology and reduced order modeling, *Structural and Multidisciplinary Optimization* 47 (6) (2013) 821–837. doi:10.1007/s00158-012-0859-4.

595 URL <https://link.springer.com/article/10.1007/s00158-012-0859-4>

- 600 [27] O. Zahm, A. Nouy, Interpolation of inverse operators for preconditioning parameter-dependent equations, *SIAM Journal on Scientific Computing* 38 (2) (2016) A1044–A1074.

- [28] R. G. Ghanem, R. M. Kruger, Numerical solution of spectral stochastic finite element systems, *Computer Methods in Applied Mechanics and Engineering* 129 (3) (1996) 289–303. doi:10.1016/0045-7825(95)00909-4.

605 URL <http://www.sciencedirect.com/science/article/pii/0045782595009094>

- [29] J. Riccius, O. Haidn, E. Zametaev, Influence of Time Dependent Effects on the Estimated Life Time of Liquid Rocket Combustion Chamber Walls, in: 40th AIAA/ASME/SAE/ASEE Joint Propulsion Conference and Exhibit, American Institute of Aeronautics and Astronautics. doi:10.2514/6.2004-3670.

610 URL <https://arc.aiaa.org/doi/abs/10.2514/6.2004-3670>

- [30] J. Riccius, E. Zametaev, O. Haidn, C. Gogu, LRE Chamber Wall Optimization Using Plane Strain and Generalized Plane Strain Models, in: 615

42nd AIAA/ASME/SAE/ASEE Joint Propulsion Conference & Exhibit,
American Institute of Aeronautics and Astronautics. doi:10.2514/6.
2006-4366.

URL <https://arc.aiaa.org/doi/abs/10.2514/6.2006-4366>

- 620 [31] A. J. M. Ferreira, MATLAB Codes for Finite Element Analysis, Solid Me-
chanics and Its Applications, Springer Netherlands, 2009.

URL [//www.springer.com/gp/book/9781402091995](http://www.springer.com/gp/book/9781402091995)